

Impact mechanisms of shallow cumulus convection on tropical climate dynamics *

ROEL A. J. NEGGERS[†] J. DAVID NEELIN AND BJORN STEVENS

Department of Atmospheric and Oceanic Sciences, University of California at Los Angeles

(October 20, 2005)

ABSTRACT

Subtropical shallow cumulus convection is shown to play an important role in tropical climate dynamics through a chain of indirect feedbacks. It is found that the presence of shallow convection in the subtropics contributes to setting the width and intensity of oceanic intertropical convergence zones (ITCZs), a mechanism here termed the *shallow cumulus humidity throttle*. These conclusions are reached after investigations based on a tropical climate model of intermediate complexity, with sufficient vertical degrees of freedom to capture i) boundary layer physics and ii) feedbacks between tropospheric humidity and deep convection. Using this modeling framework, the mechanisms of interaction between small-scale shallow cumulus convection and large-scale tropical and subtropical climate dynamics are identified and quantified. A simple first-order parameterization for shallow cumulus convection is used in which the time scale of shallow cumulus adjustment can be varied to assess sensitivity. A moist static energy budget analysis is then performed that reveals the chains of relevant feedback mechanisms acting in the tropics.

The first direct impact of reduced shallow cumulus convection is to increase boundary layer humidity in the subtropics. This locally reduces surface evaporation and suppresses tropospheric humidity. Horizontal transport of this drier air by humidity transients and dry intrusions significantly reduces the precipitating deep convection at the edges of the oceanic convection zones. As a result, the temperature is reduced by several degrees throughout the tropics. In turn, the combination of this temperature change and the subtropical drop in water vapor path triggers a compensating increase in net longwave warming and surface heat flux. In the central axis of the oceanic convection zones this acts to increase the moist static energy forcing, which results in stronger large-scale convergence producing more intense precipitation.

1. Introduction

Shallow cumulus is widespread in the subtropics and tropics, and can have considerable importance from the perspective of climate system dynamics. While a number of in situ field-experiments in the past have revealed much about shallow convection itself, the model study by Tiedtke et al. (1988) was one of the first attempts to quantify the impact of shallow cumulus convection on global tropical climate. The occasion was the introduction of a shallow convection scheme in the forecast model of the European Centre for Medium-range Weather Forecasts (ECMWF). The main conclusions were that locally, vertical transport by shallow cumulus dries the subcloud layer, thus enhancing surface evaporation. Interestingly, they also found that shallow cumulus convection significantly impacts the larger scale dynamics and model climate. They reported an intensified ITCZ, said to be due to the extra convergence of

humidity. Changes in the global thermal/humidity state also were reported. Later studies using general circulation models (GCM) have more or less confirmed these findings (Slingo et al. 1994; Gregory 1997; Jakob and Siebesma 2003).

These results justify studies on the interaction mechanisms between subtropical shallow cumulus and the tropical convection zones as part of the large scale circulation. Horizontal humidity advection is likely to be important in this interaction, as it carries air of a certain humidity state from the subtropics towards the ITCZ. Transients are known to have strong impacts on horizontal moisture transport in the free troposphere, featuring high moisture air masses in the shape of elongated filaments travelling over long distances (Newell et al. 1992; Newell and Zhu 1994; Pierrehumbert and Yang 1993). The reverse of moist plumes, called dry intrusions, also occur (e.g. Parsons et al. 2000). While the atmospheric boundary layer (ABL) moisture is strongly restored towards saturation by the surface fluxes, the free tropospheric moisture is largely decoupled from the ABL except where convection occurs. As a result, advected dry plumes can penetrate large distances. Deep convective cloud height and precipitation are observed to be sig-

*This is Inst. of Geophysics and Planetary Physics contribution number 6245

[†]Current affiliation: European Centre for Medium-range Weather Forecasts *Corresponding author address*: R. A. J. Neggers, ECMWF, Shinfield Park, Reading, Berkshire, RG2 9AX, UK. E-mail: Roel.Neggers@ecmwf.int

nificantly reduced and replaced by shallower convection in situations of strong advective drying in the free troposphere. This sensitivity of deep convection to tropospheric humidity has also been demonstrated in cloud resolving models (Derbyshire et al. 2004). It can thus be argued that shallow convection affects deep convection locally by moistening the lower troposphere above the subcloud ABL.

Besides this local impact, deep convection in the tropical ITCZs is also affected remotely by shallow cumulus, due to its persistent occurrence in the subtropical Tradewind regions. Horizontal moisture advection has been found to affect deep convection on the margins of the convective zones in mechanisms that involve feedbacks with the large scale circulation (Neelin et al. 2003; Chou and Neelin 2004). Tradewind cumulus can be argued to act as a 'valve' on the vertical humidity flux at the top of the subcloud mixed layer (Neggers et al 2005). Here we postulate that shallow convection, by controlling the humidity in the lower troposphere that is advected into the ITCZ margins, participates in interactions with the large scale circulation that impact the ITCZs. We term this the "shallow convective humidity throttle" (*Cu-q throttle*), since shallow convection controls the fuel available to the deep convective zones.

In investigating the role of shallow cumulus in large scale climate, we use an intermediate complexity climate model, the Quasi-equilibrium Tropical Circulation Model [QTCM, Neelin and Zeng (2000, NZ00 hereafter); Zeng et al. (2000)]. It has been shown to reproduce tropical climatology to a reasonable degree (Zeng et al. 2000). In this study, an extra degree of freedom for humidity is introduced in the model representing an atmospheric boundary layer. Accordingly, the free troposphere gets decoupled from the atmospheric boundary layer, to a degree which is set by the local convective activity. We hope thus to reproduce the observed free tropospheric humidity transients in the QTCM.

The introduction of the boundary layer implies changes in the QTCM convection scheme. A simple first-order shallow convection scheme is embedded in an already existing Betts-Miller framework for deep convection. As for deep convection, shallow cumulus intensity will be defined by a typical adjustment timescale for this type of convection. Apart from shallow and deep convection, this change also implies that an analogue of cumulus congestus now occurs in the model as well. These three types of convection dominate the cloud type distribution in the tropics (Johnson et al. 1999).

In analyzing interactions with the large scale flow we use the moist static energy (MSE) framework (Neelin and Held 1987). While the convective heating term and the convective moisture sink term dominate in the heat

and moisture budget equations respectively, they cancel in the MSE equation (e.g. Yanai et al. 1973). This can aid insight into the smaller but controlling terms in the large scale budget. Under certain conditions the MSE equation can even be used as governing equation for the large scale flow in the tropics (Zeng et al. 2000). The moist static energy budget equation has been used successfully to relate tropical temperature, humidity, precipitation and divergence anomalies in tropical climate phenomena such as El Niño and teleconnections (e.g. Su et al. 2003; Su and Neelin 2002, 2003; Chou and Neelin 2004). By calculating MSE budgets it should be possible to trace and quantify the interactions between model climate and shallow convection. Changes in the large scale circulation can be examined in terms of changes in thermodynamic and diabatic forcings. This facilitates isolating the dominant physical processes/ transports.

To summarize, using the QTCM framework the sensitivity of model climate to tropospheric humidity transients and shallow cumulus convection is studied. Section 2 briefly describes the QTCM and the introduction of a boundary layer in the model, and in Section 3 the associated changes in the convection scheme are formulated. Section 4 discusses the methodology of the study, consisting of a series of runs with varying shallow cumulus intensity. In Section 5 the associated changes in mean tropical climatology are presented, while in Section 6 the QTCM humidity field is examined in more detail. In Section 7 the tropical MSE budget is explored, revealing the nature of the interaction between shallow cumulus and the large scale circulation. In Section 8, implications are discussed.

2. QTCM

a. Short description of the standard model

The full description of the quasi-equilibrium tropical simulation model (QTCM) is given by NZ00 and Zeng et al. (2000). One of the core assumptions at the basis of the QTCM which greatly simplifies the tropical dynamics is the assumption of a fixed vertical temperature structure. In quasi-equilibrium conditions the relatively short adjustment timescale of deep convection keeps the tropical temperature close to the moist adiabat. Through the pressure gradient term, this assumed vertical structure determines the basis function for the baroclinic wind component.

Convection in the single basis function (1BF) QTCM is by definition precipitating, as it considers only column-averages. Only the loss of humidity to the surface is required in that setup, and vertical redistribution of moisture within the column itself is not considered.

Deep convection is modeled using the adjustment framework of Betts (1986) and Betts and Miller (1986) (collectively BM86 hereafter). It keeps the temperature profile close to the moist adiabat by using a relatively fast adjustment timescale (as compared to that of the large scale circulation), hence the words "quasi-equilibrium" in the name QTCM. A short summary of the relevant elements for this paper is given here; for detailed description see NZ00.

Conservation of energy implies that the column-average latent heat release by deep convection $\langle Q_c \rangle$ is equal to the net humidity sink due to precipitation $\langle Q_q \rangle$,

$$\langle Q_c \rangle = -\langle Q_q \rangle. \quad (1)$$

Remaining compatible with the notation used in NZ00 both $\langle \cdot \rangle$ and $\hat{\cdot}$ refer to a column-average. BM86 expressed this apparent heat source and sink in the form of a relaxation equation,

$$\langle Q_c \rangle = \frac{\langle T^c - T \rangle}{\tau_{dp}}, \quad \text{and} \quad \langle Q_q \rangle = \frac{\langle q^c - q \rangle}{\tau_{dp}}, \quad (2)$$

where T is temperature in energy units with heat capacity c_p absorbed, q is moisture in energy units with latent heat capacity L absorbed, and the superscript c denotes their convective adjustment profile. τ_{dp} , the associated convective adjustment timescale, is assumed to be on the order of two hours. The term $\langle T^c - T \rangle$ is a measure of convective available potential energy (CAPE), representing that part of the real CAPE which is actually converted into latent heat by precipitation loss. In this paper it will be indicated by CAPE1, to stay compatible with the previous QTCM papers.

Writing T^c and T each in terms of a constant reference profile, $T_r^c(p)$ and $T_r(p)$, and a vertical basis function $a_1(p)$ associated with convective quasi-equilibrium, gives

$$T = T_r + T_1(x, y, t) a_1(p), \quad (3)$$

$$T^c = T_r^c + T_1^c(x, y, t) a_1(p). \quad (4)$$

Applying this to (2) and rearranging gives \hat{T}_1^c as a function of the thermodynamic state $\{T, q\}$ of the column,

$$\hat{A}_1 \hat{T}_1^c + \hat{q}^c(T_1^c) = \hat{a}_1 \hat{T}_1 + \hat{q} - (\hat{T}_r^c - \hat{T}_r). \quad (5)$$

As in NZ00, following the BM86 moisture closure it is assumed that q^c is a specified function of the saturation humidity profile,

$$q^c = \alpha(p) q_{sat}, \quad (6)$$

which can be written as a function of T^c and p . Obtaining \hat{T}_1^c and \hat{q}^c using (5) then enables calculation of $\langle Q_c \rangle$ and $\langle Q_q \rangle$, which appear in the prognostic heat and moisture equations as the convective tendencies.

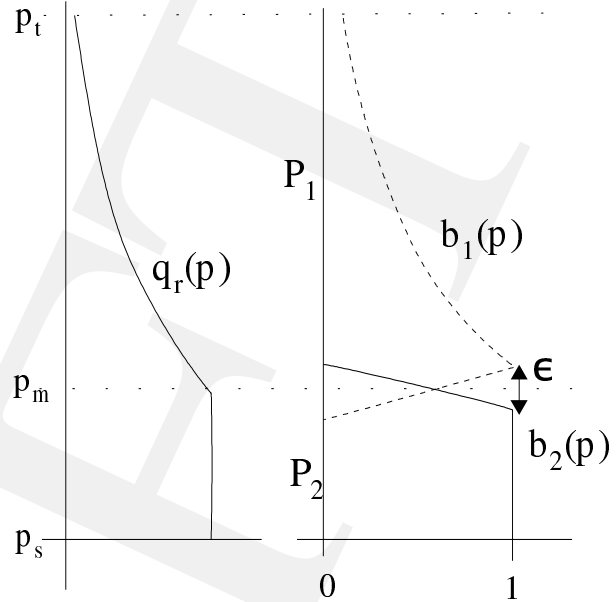


FIGURE 1: The configuration of the vertical structure functions b_k . Perturbations of humidity are strongest in the subcloud mixed layer and in the lower troposphere.

b. A second basis function for humidity

The main reasons for introducing an atmospheric boundary layer in the QTCM have been outlined in the introduction. The presence of a shallow layer between the free troposphere and the surface strongly affects the surface sensible and latent heat fluxes, as well as the climatology of tropospheric humidity. Another related issue is the typically high variability present in observed vertical humidity profiles (e.g. Liu et al. 1991). A decoupled two-layer system for humidity in the QTCM, representing an atmospheric boundary layer below a free troposphere, might capture typical advective characteristics of the tropospheric humidity field (e.g. Pierrehumbert and Yang 1993). While the boundary layer will be strongly tied to the SST through the surface evaporation, the relatively deep free tropospheric layer will be dominated by horizontal advection outside of deep convective areas.

The atmospheric humidity field is far less constrained than the temperature field, which is affected by both convection and wave dynamics. Tropospheric temperature is strongly tied to the large scale dynamics through the pressure gradient term, a concept which is explicitly used in the QTCM formulation. In contrast, the tropospheric humidity field behaves much more like a passive scalar in the absence of deep convection. The discretization of the moisture vertical structure is essentially independent of that for temperature and velocity. Thus introduction of a second degree of freedom in moisture while

retaining the same structure for the rest of the model provides a clear case to isolate moisture impacts.

c. 2BF formulation

For moisture q we thus extend the QTCM 1BF standard model to a two basis function (2BF) version. As described by NZ00 for the 1BF case, a Galerkin approximation is made around a reference climatological moisture profile $q_r(p)$,

$$q(x, y, p, t) = q_r(p) + \sum_{k=1}^2 b_k(p) q_k(x, y, t), \quad (7)$$

where k is the mode-index, b_k is the vertical structure function of each mode, and q_k is a time-dependent scalar field. There are thus two prognostic equations for moisture.

The choice of the vertical structure functions b_k depends on the problem of interest. As our purpose is to introduce a boundary layer for humidity, we choose each of the two functions to cover separate layers, see Fig. 1. The first function $b_1(p)$ covers the free troposphere without the atmospheric mixed layer (of constant depth of 100 mbar), which is covered by the second function $b_2(p)$. Within its pressure-depth P_k each function b_k is non-zero, while outside of it it is zero. An infinitesimal small overlap ϵ at mixed layer top (at 900 mbar) is introduced to facilitate derivations (see Appendix A), letting $\epsilon \rightarrow 0$. Hereafter a vertical average over layer k is indicated as $\hat{\cdot}_k \equiv \langle \cdot \rangle_k$.

An essential concept of the QTCM is that vertical integration is performed before time-integration, while still maintaining as much vertical non-linearity as possible through pre-calculated constants. We thus work with a subcloud mixed layer of constant depth. While a simplification of reality, observations show that the subcloud mixed layer height in the subtropics is indeed remarkably constant (Riehl et al. 1951, e.g.).

Note that the vertical structure functions b_k represent the vertical distribution throughout each layer of the departures of the actual moisture profile q from a climatological reference profile q_r . Figure 1 shows that while in the subcloud mixed layer (layer 2) the structure function is constant, in the free troposphere (layer 1) the largest absolute changes in humidity take place in the lower troposphere. This enables large moisture differences to exist between layer 1 and layer 2 at cloud base, while simultaneously the upper tropospheric moisture is still close to its characteristic low value.

The technical details of the implementation of the second basis function in the QTCM is relatively straightfor-

ward, and follows the notation of NZ00. A short description can be found in Appendix A.

3. The 2BF convection scheme

The introduction of the boundary layer implies modifications in the QTCM convection scheme, including redistribution of humidity between the ABL and the free troposphere, as well as precipitation. Instead of one type of convection, now three modes can be distinguished: deep convection, cumulus congestus and shallow convection, as schematized in Fig. 2 and defined below. These three types of convection are observed to dominate the cloud type distribution in the tropics (Johnson et al. 1999). The new convective modes are produced by extending in the Betts-Miller framework for deep convection of the 1BF QTCM. As for deep convection, shallow cumulus intensity will be defined by a typical adjustment timescale.

a. Deep convection

In the 2BF setup, deep convective CAPE1 is calculated in the same way as in the 1BF setup, in the sense that the total water vapour path through the whole column is still fed into energy constraint (5) to get \hat{T}_1^c and \hat{q}_c . The difference is that \hat{q} now stands for the effective vertically averaged humidity over two layers instead of a single tropospheric layer,

$$\hat{q} = \sum_{k=1}^2 \frac{P_k}{P_T} \hat{q}_k. \quad (8)$$

The presence of a second degree of freedom for humidity in the model thus affects the deep convective precipitation rate $\langle Q_c \rangle$. The apparent humidity sink now consists of two terms representing the two separate layers,

$$\langle Q_c \rangle = -\langle Q_q \rangle \equiv -\sum_{k=1}^2 \frac{P_k}{P_T} \langle Q_q \rangle_k. \quad (9)$$

As the shallow boundary layer is always relatively moist, determined in large part by the SST, convection typically acts to dry out the boundary layer ($\langle Q_q \rangle_2 < 0$). Under situations favorable to intense deep convection, the lower troposphere has moisture convergence balanced by the convective moisture sink, so $\langle Q_q \rangle_1 < 0$ as well. However, situations with low tropospheric humidity can now reduce $\langle Q_c \rangle$ through $\langle Q_q \rangle_1 > 0$, a situation corresponding to free tropospheric moistening. This suppresses surface precipitation. For a sufficiently dry lower troposphere $\langle Q_c \rangle$ can even become zero, in which case surface precipitation completely switches off and non-precipitating cumulus (Section 3c) takes over.

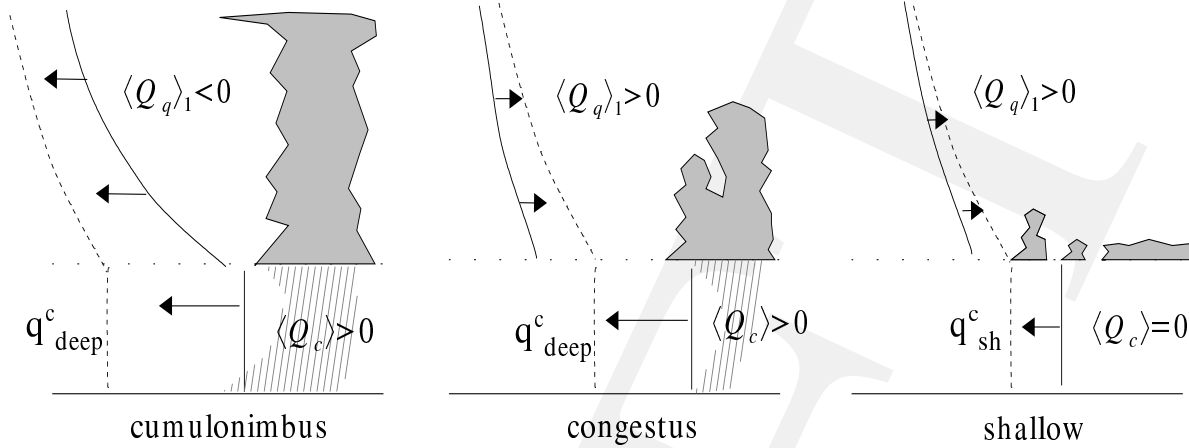


FIGURE 2: An overview of three possible scenarios for the two apparent moisture sink terms $\langle Q_q \rangle_k$ in the 2BF setup. The dashed line indicates the convective adjustment profile for moisture, q^c_{deep} for deep convection and q^c_{sh} for shallow cumulus convection. The solid line represents the actual humidity profile. The name “congestus” is used as a shorthand term for precipitating shallow convection.

b. Congestus

A separate regime in precipitating convection can now be distinguished in the model. The situation can exist in which net surface precipitation occurs but in which convection still moistens the free troposphere,

$$\langle Q_c \rangle > 0 \quad (10)$$

$$\langle Q_q \rangle_1 > 0, \quad (11)$$

see Fig. 2. This corresponds to *precipitating shallow cumulus* or *cumulus congestus* for short, given the resemblance to a regime with substantial cumulus congestus. Note that (5) implies T^c is adjusted to a smaller value when the tropospheric air is dry than when it is wet. Thus the impact of free tropospheric humidity affects the buoyancy term ($T^c - T$), and thus the precipitation.

c. Shallow cumulus

When $CAPE_1$ is equal to or smaller than zero, no precipitating convection is expected in this model. Nevertheless, redistribution of humidity can still take place between the two layers, without creating net surface precipitation:

$$\langle Q_c \rangle = 0 \quad (12)$$

$$P_2 \langle Q_q \rangle_2 = -P_1 \langle Q_q \rangle_1. \quad (13)$$

This situation represents low, non-precipitating convection such as *shallow cumulus convection*. The extra condition (12) was also used by BM86 in their shallow convection scheme.

In the Betts-Miller framework, shallow convection is expressed as a relaxation term acting on the excess of mixed layer humidity over its adjustment value q^c_{sh} ,

$$\langle Q_q \rangle_2 = \frac{\langle q^c_{sh} - q \rangle_2}{\tau_{sh}} \quad (14)$$

where τ_{sh} represents the typical time in which shallow cumulus vertical transport tends to reduce humidity differences between boundary layer and free troposphere. Condition (13) implies

$$\hat{q}^c_{sh} = \hat{q} \quad (15)$$

which shall hereafter be referred to as \hat{q}^c_{sh} , the adjustment value for shallow convection. This represents the state towards which the system is driven by pure internal vertical redistribution. Writing the vertical structure of q^c_{sh} in terms of the same BF used for q , gives

$$q^c_{sh}(x, y, p, t) = q_r(p) + \sum_{k=1}^2 b_k(p) q^c_{sh,k}(x, y, t). \quad (16)$$

We further assume that the shallow cumulus mixing drives the moisture in the free troposphere to a profile such that the values at cloud base are equal to those in the mixed layer, so $q^c_{sh,1} = q^c_{sh,2}$. With (15), this yields the shallow adjustment projection coefficients $q^c_{sh,k}$,

$$q^c_{sh,2} = q^c_{sh,1} = \frac{P_1 \hat{b}_1 q_1 + P_2 \hat{b}_2 q_2}{P_1 \hat{b}_1 + P_2 \hat{b}_2}, \quad (17)$$

a diagnostic function of q_1 and q_2 . Comparing to the deep convective moisture closure (6), this implies that

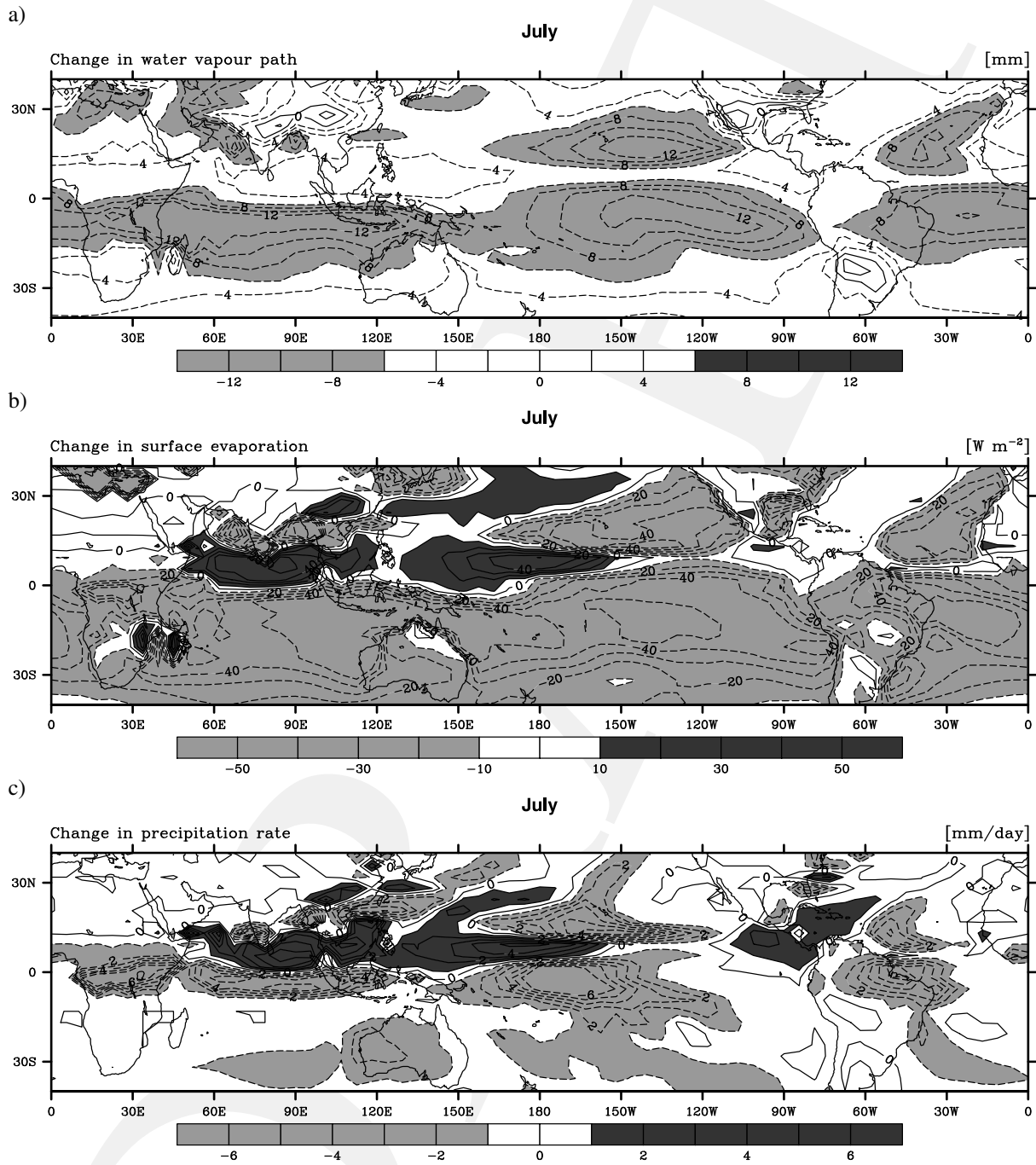


FIGURE 3: The change in the July climatology of a) water vapour path [mm], b) surface evaporation [W m^{-2}] and c) precipitation rate [mm day^{-1}] for the $\tau_{sh} = 200000\text{s}$ run minus the $\tau_{sh} = 1200\text{s}$ run.

for non-precipitating cumulus, the degree of subsaturation is set by mixing processes, rather than specified.

In order to derive a typical first-order value for τ_{sh} , one can convert (14) into flux units by multiplying with height and then make the mass flux approach (e.g. Ooyama 1971; Yanai et al. 1973; Betts 1975) for the left-hand side. This gives

$$z_b \langle Q_q \rangle_2 \approx -m (q_t^{core} - q_t^{env})_b. \quad (18)$$

Here z_b is the subcloud mixed layer depth and m is the shallow cumulus mass flux at z_b . The mass flux acts to reduce the total specific humidity difference between the cloud environment q_t^{env} and the active cloudy thermals q_t^{core} by convective overturning. In the rising undiluted parcel interpretation, these rising thermals still have specific humidity levels very close to subcloud mixed layer values. Accordingly, it makes sense to scale the cloud excess at cloud base with the excess over the shallow adjustment profile,

$$(q_t^{core} - \bar{q}_t)_b \sim (q - q_{sh}^c)_2. \quad (19)$$

Using $z_b = 1000$ m and $m = 0.01$ m s⁻¹ as typical values for Tradewind cumulus (e.g. Siebesma and Cuijpers 1995) and combining (14)-(19), this gives

$$\tau_{sh} = \frac{z_b}{m} \sim 1 \cdot 10^5 s. \quad (20)$$

This mass flux based shallow convective adjustment timescale serves as a reference value in the sensitivity test discussed in the next sections.

Of course τ_{sh} could be related to the state of the model, as is implicitly done in a mass flux framework. This would result in a spatially varying shallow adjustment timescale. These issues are explored in a subsequent paper. Recent research suggests that a strong negative feedback mechanism acts between mass flux and boundary layer humidity at shallow cumulus cloud base, acting as a valve on the upward transport of heat and moisture from the subcloud mixed layer (Neggers et al 2005).

d. Shallow cumulus humidity throttle

At this point some impact mechanisms of shallow cumulus convection on the tropical climate system in the QTCM can a priori be distinguished. Locally, at the edges of the ITCZ, during a dry tropospheric intrusion shallow cumulus will temporarily replace precipitating convection. Only after shallow convection has moistened the troposphere sufficiently can deep convection again occur. This corresponds to a situation such as observed by Parsons et al. (2000) during the Tropical

Ocean and Global Atmosphere (TOGA) Coupled Ocean-Atmosphere Response Experiment (COARE).

Remotely, in the subtropical Tradewind regions, shallow cumulus continuously maintains the humidity levels of the lower free troposphere by vertical humidity transport at cloud base. This humidity is then advected horizontally into the ITCZ, where it helps maintain deep convective occurrence and intensity. Advection of less-moistened air, on the other hand, tends to reduce convection at the margins of the ITCZs (Chou and Neelin 2004).

This set of feedbacks, in which the intensity of shallow convection creates both local and remote impacts by its control of tropospheric moisture q , is what we term the "shallow cumulus humidity throttle" (or *Cu-q throttle*) mechanism. Here we test impacts of the Cu-q throttle by varying shallow cumulus parameters. We then diagnose the chain of feedbacks at larger scales.

4. Methodology

A sensitivity test is performed on the QTCM climatology for the gradual decoupling of the boundary layer from the free troposphere. This is done through varying the value of a spatially homogeneous τ_{sh} . Although a constant τ_{sh} might not be realistic, it does i) reveal the first-order impacts of shallow cumulus activity on the climate system, and ii) facilitates comparison to the original IBF QTCM. Note that a shallow cumulus mass flux model was implemented in the QTCM by Neggers et al (2005), implying a spatially varying τ_{sh} .

Over a series of separate runs the shallow convective adjustment timescale τ_{sh} is altered, spanning its realistic range between 0.5 and 2.0 times its typical value as was derived in (20). This range is considered to be typically encountered in convection schemes in GCMs. For the sake of completeness, the range is extended towards 0.012 times (20) (the model integration timestep), corresponding to a strongly mixed atmosphere in humidity in which the free troposphere is completely coupled to the boundary layer. Sections 5 - 7 deal with the results of this sensitivity test, using the MSE framework.

Each run covers 17 years, over which averages are also calculated. The observed sea-surface temperature (SST) is specified as a boundary-condition. The impacts of an interactive oceanic mixed layer in this problem are summarized in Section 7e.

5. Results: mean climatology

Comparing the series of runs with different τ_{sh} reveals significant changes in the tropical and subtropical climatology. Figure 3a shows that the total column wa-

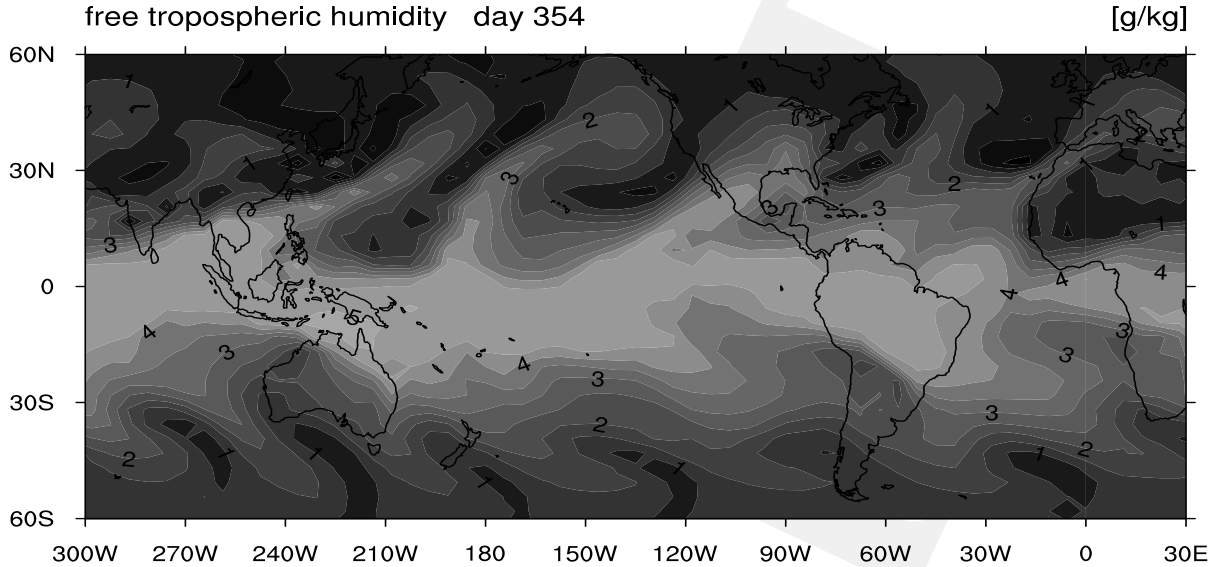


FIGURE 4: Example of the free tropospheric humidity field \hat{q}_1 [g kg^{-1}] for a 1-day average on a December day in 1982, of the model run with $\tau_{sh} = 1 \cdot 10^5 \text{s}$.

ter vapour path drops everywhere as τ_{sh} increases. This is most significant in the subtropics, where subsidence associated with the Hadley Circulation is effective in drying the free troposphere. As the shallow convective transport is decreased, the mixed layer moistens and the free troposphere dries out. Roughly comparing to SSMI observations (not shown here) reveals that the general structure of the QTCM water vapour path field becomes more realistic, with narrower ITCZs and drier subtropics as τ_{sh} increases from short values to values on the order of a day.

The associated drop in surface evaporation is shown in Fig. 3b. The more humid boundary layer with increasing τ_{sh} is the direct cause for this reduction. This finding is in agreement with the results of Tiedtke et al. (1988). In contrast, in the central axis of the oceanic ITCZs the surface evaporation has increased.

The change in precipitation rate is plotted in Fig. 3c. In general, the edges of the precipitating ITCZ area suffer a significant decrease in precipitation rate, up to 5 mm/day in some areas. In contrast, the core axes of the oceanic ITCZs experience an increase of up to 6 mm day⁻¹. The spatial pattern of the positive precipitation matches that of the positive evaporation change in Fig. 3b, although the local amplitude of precipitation (noting $1 \text{ mm day}^{-1} = 28 \text{ W m}^{-2}$) is substantially larger. Comparing Fig. 3c to Fig. 3a shows that the areas of significant decrease in precipitation rate always correspond to lower water vapour paths. Precipitation reductions over the continents are approximately as strong as over the

oceans, although precipitation increases tend not to occur over land.

Only the month of July is shown here, but these results are similar for all months of the year (not shown, except in Fig. 14) with the spatial patterns moving according to the seasonal movements of the convection/subsidence regions. To optimize readability and reduce the number of plots, only July will be discussed. The seasonal dependence of the climate mechanisms involved is addressed in the discussion in Section 8.

6. Humidity transients

The 2BF QTCM convection scheme as described in Section 3 implies that precipitating deep convection is sensitive to tropospheric humidity. The fact that the precipitation decrease at the edges of the ITCZ with increasing τ_{sh} coincides with significantly lower water vapour paths suggests that this feedback is indeed occurring in the model.

The QTCM tropospheric humidity field during the run with $\tau_{sh} = 1 \cdot 10^5 \text{ s}$ on a mid December day is shown in Figure 5. The humidity field is far from smooth, featuring relatively thin, elongated plumes of moist and dry air. These transients cover a latitude range on the order of 40 degrees, and the dry air seems able to reach all the way to the equator on some occasions. The horizontal gradients between moist and dry air are often very large and abrupt. In general, these characteristics agree quite well with typical daily SSMI observations (not shown).

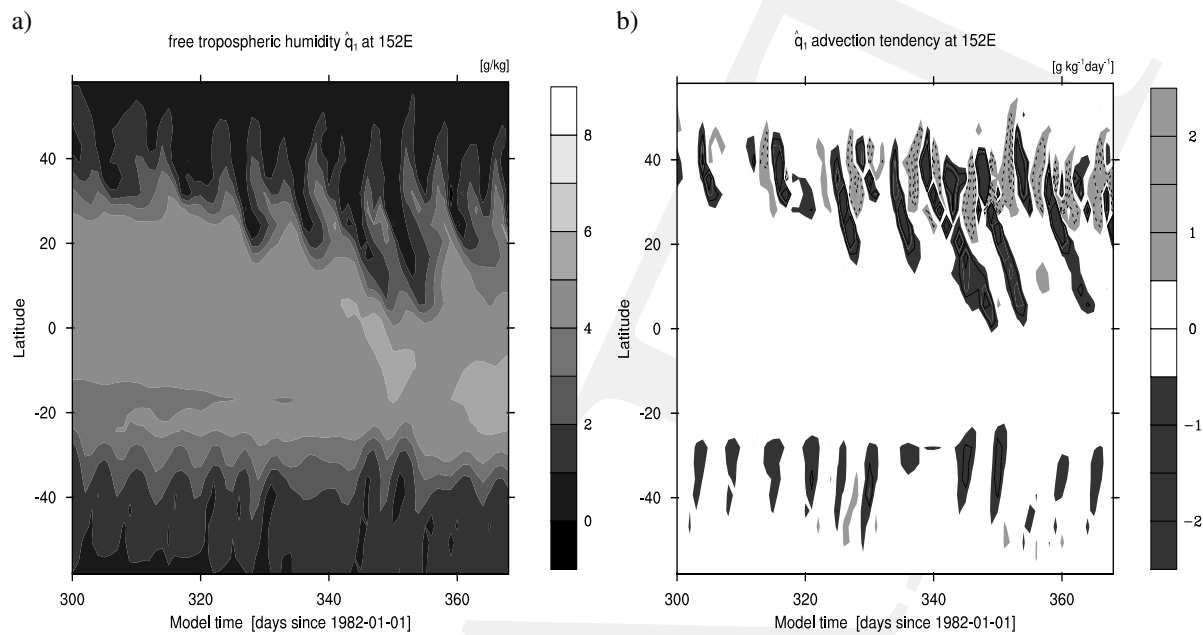


FIGURE 5: Latitude-time plots of a) free tropospheric humidity \hat{q}_1 [g kg^{-2}] and b) the free tropospheric humidity tendency by advection [$\text{g kg}^{-1} \text{day}^{-1}$], at longitude $151E$ for the period of November-December in 1982, for the model run with $\tau_{sh} = 1 \cdot 10^5 \text{s}$.

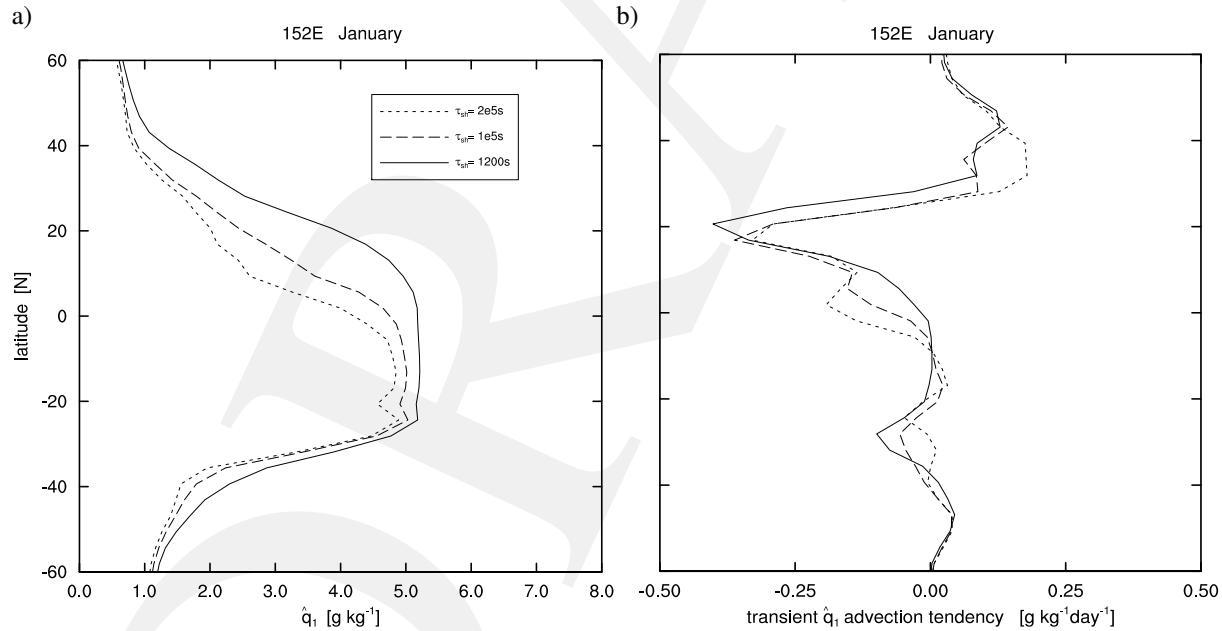


FIGURE 6: Meridional cross-section in the Western Pacific at longitude $151E$ through a) the free tropospheric humidity \hat{q}_1 and b) the transient advection field in the free troposphere. Each line represents a separate run, with $\tau_{sh} = 1.2 \cdot 10^3 \text{s}$, $1 \cdot 10^5 \text{s}$ and $2 \cdot 10^5 \text{s}$, respectively.

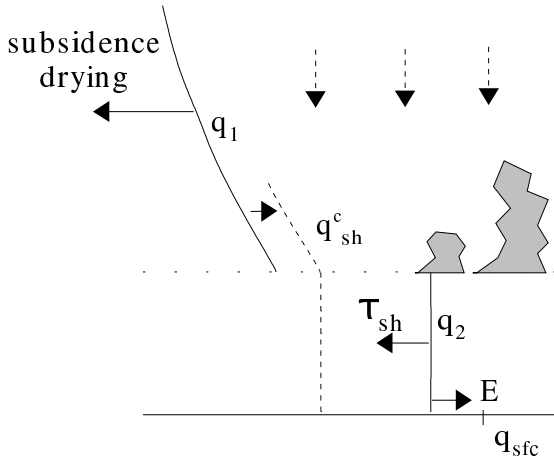


FIGURE 7: Processes acting on humidity in the 2BF setup for non-precipitating subsidence situations. Each process is represented by a solid arrow. The symbols are explained in the text. The dotted line represents the shallow adjustment humidity profile q_{sh}^c . While surface evaporation E acts to moisten the boundary layer, shallow convection τ_{sh} acts to dry it out. In the free troposphere, shallow convection moistens while large scale subsidence (dotted arrows) dries.

The nature of the time development of the tropospheric humidity field is revealed by Fig. 5, which shows the tropospheric humidity and associated advective tendency for a one-month period. The location corresponds to the TOGA-COARE area in the Western Pacific warm pool, where the well-studied dry-intrusion event took place as documented by Parsons et al. (2000). It is evident that the transients are of advective nature. The transient activity is most intense at the northern side of the warm pool. The reason for this is the relatively close proximity of mid-latitude disturbances to the convection zone in northern-hemisphere winter, resulting in intense interaction and exchange between the mid-latitudes and the tropical belt in the Warm Pool (Lin et al. 2000).

Figure 6a shows a latitude cross-section of the free tropospheric humidity (q_2) climatology. The location and season correspond to Fig. 5. The changes in free tropospheric humidity with τ_{sh} are most significant at the northern side of the warm pool. To quantify the relative importance of advective humidity transients in this process, the total advective humidity tendency is split up into a mean and transient part,

$$(\mathbf{v} \cdot \nabla q)_{trans} = \overline{\mathbf{v} \cdot \nabla q} - \mathbf{v} \cdot \nabla \bar{q}. \quad (21)$$

The overbar represents a climatological average as a function of season. The transient part (left hand side) is obtained as the residual of the two terms of the right hand side, and represents all product-terms including a perturbation term. Figure 6b shows a cross-section of the

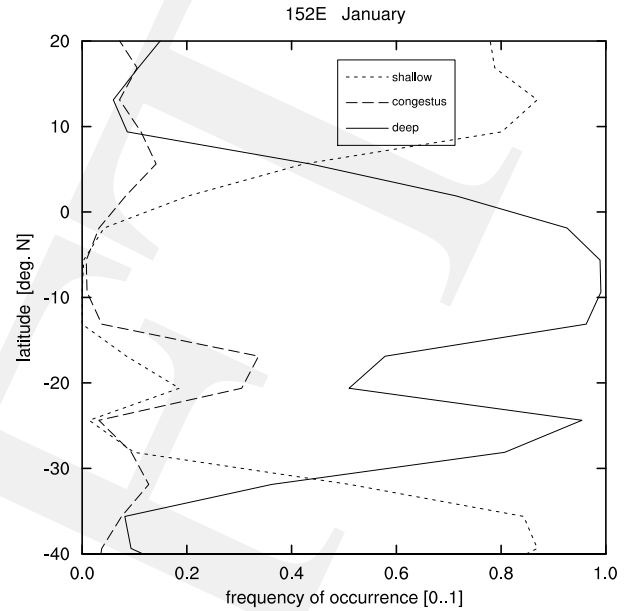


FIGURE 8: Monthly mean climatological frequency of occurrence of the three modes of convection in January, on a cross-section at 152E for $\tau_{sh} = 2 \cdot 10^5$ s.

transient advection. It peaks roughly where the meridional humidity gradient is strongest. Clearly, at about 5S-10N, the transient dry advection reaches further into the tropical humidity belt with weakening shallow cumulus (increasing τ_{sh}). On the other hand, further north at about 30-40N there is an increased moistening tendency, pointing to moist plumes bringing humidity out of the warm pool. The sign and location of the transient advection climatology in Fig. 6 correspond well with the behaviour of the individual events captured in Fig. 5.

Several reasons exist for the dry humidity transients to reach further into the ITCZ for larger τ_{sh} . First, the decoupling of the free troposphere from the boundary layer allows for horizontal advection to dominate the humidity budget; effectively, there is weaker damping by shallow convection of dry anomalies created by advection, extending their lifetime. Second, the tropospheric humidity in the source of these intrusions (the subtropics) has dropped significantly by large scale subsidence due to the increased τ_{sh} , as schematized in Fig. 7; shallow convection is less able to maintain the moisture in the troposphere against subsidence.

During an intrusion of dry air into the edge of the ITCZ, precipitation is temporarily replaced by shallow cumulus or cumulus congestus, until the tropospheric moisture is restored to such a degree that deep convection can occur again. Supporting this, Fig. 8 shows that congestus occurrence peaks at the edges of the deep convective ITCZ. Since congestus is defined in (10)-(11) as

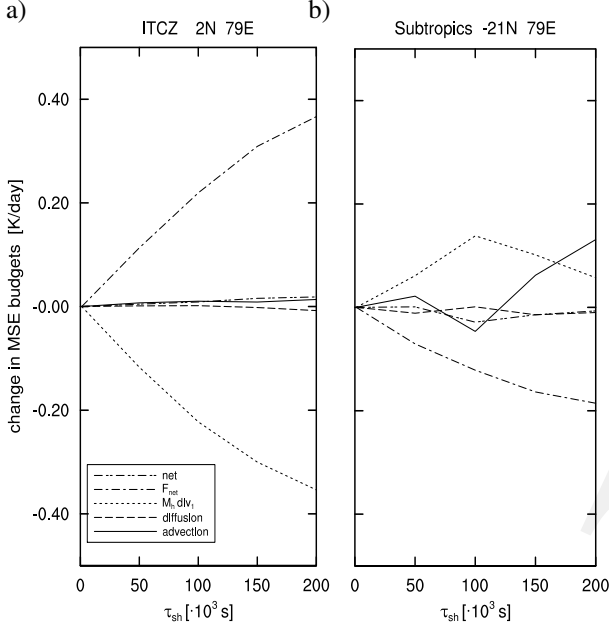


FIGURE 9: The change of the moist static energy budgets compared to the $\tau_{sh} = 1200s$ run as a function of τ_{sh} , at different locations in the Indian Ocean. The left panel shows a location inside the convection zone, the right panel a location just south of the convection zone. The acronyms refer to the terms in (23).

net surface precipitation in combination with free tropospheric moistening, this points to free tropospheric humidity decreases temporarily reducing the deep convection. The impacts are greatest at the edges of the ITCZ, where humidity advection is an important term in the tropospheric humidity budget. Although the incoming transients are temporary disturbances that typically last only a few days, they have a strong net impact on the climatology of convective precipitation at these locations.

7. Climate feedback mechanisms

Figure 3c shows that, in contrast to the ITCZ edges, the precipitation rate has increased in its core axis. In other words, with reduced shallow cumulus (increased τ_{sh}) the oceanic ITCZs get narrower but are at the same time intensified. Apparently, shallow cumulus convection affects tropical climate through more ways than just affecting horizontal humidity advection. In order to fully understand all elements of this tropical feedback mechanism we now turn to the large scale moist static energy (MSE) budget.

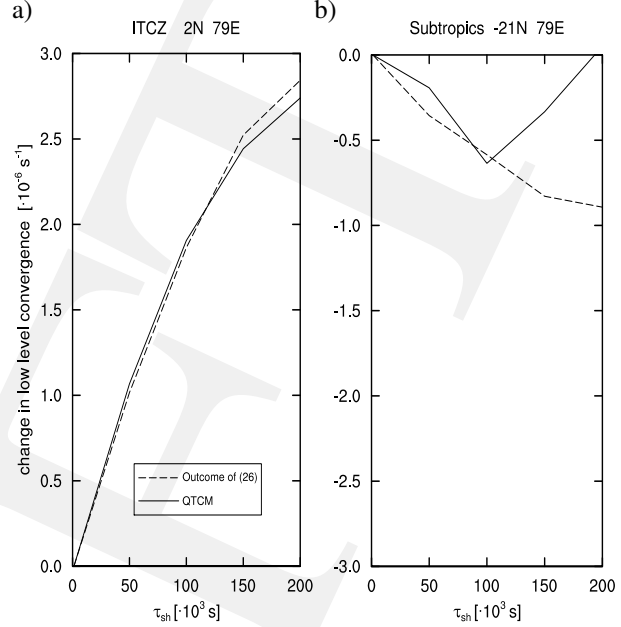


FIGURE 10: The change of the large scale low-level convergence (or upper level divergence), both model result and calculated using the simplified relation (26) which omits advection.

a) Moist static energy budgets

MSE is defined as

$$h = T + q + \phi, \quad (22)$$

(e.g. Yanai et al. 1973), where ϕ is geopotential height. The MSE budget equation is obtained by adding the prognostic equations for T and q . For our purposes we consider the perturbation equation only, which can be written as

$$\begin{aligned} \langle \partial_t(T+q) \rangle' + \langle \mathcal{D}_h(T+q) \rangle' \\ + (M\nabla \cdot \mathbf{v}_1)' = \\ (F'_{rad} + H' + E') \end{aligned} \quad (23)$$

The $\langle \rangle$ here denotes the vertical column-integral, and the prime $'$ denotes the perturbation from the reference run, in this case chosen to be the run with the smallest timescale $\tau_{sh} = 1200s$. The time-derivative is ∂_t , \mathcal{D}_h is the horizontal advection/diffusion operator, $M\nabla \cdot \mathbf{v}_1$ is the vertically integrated vertical advection term, written in terms of the *gross moist stability* M (Neelin and Held 1987) and the large scale divergence projected on the baroclinic mode $\nabla \cdot \mathbf{v}_1$. By convention, the latter is positive for low level convergence. The net static stability for convergence of large-scale motions M can be interpreted as the work that the large scale circulation

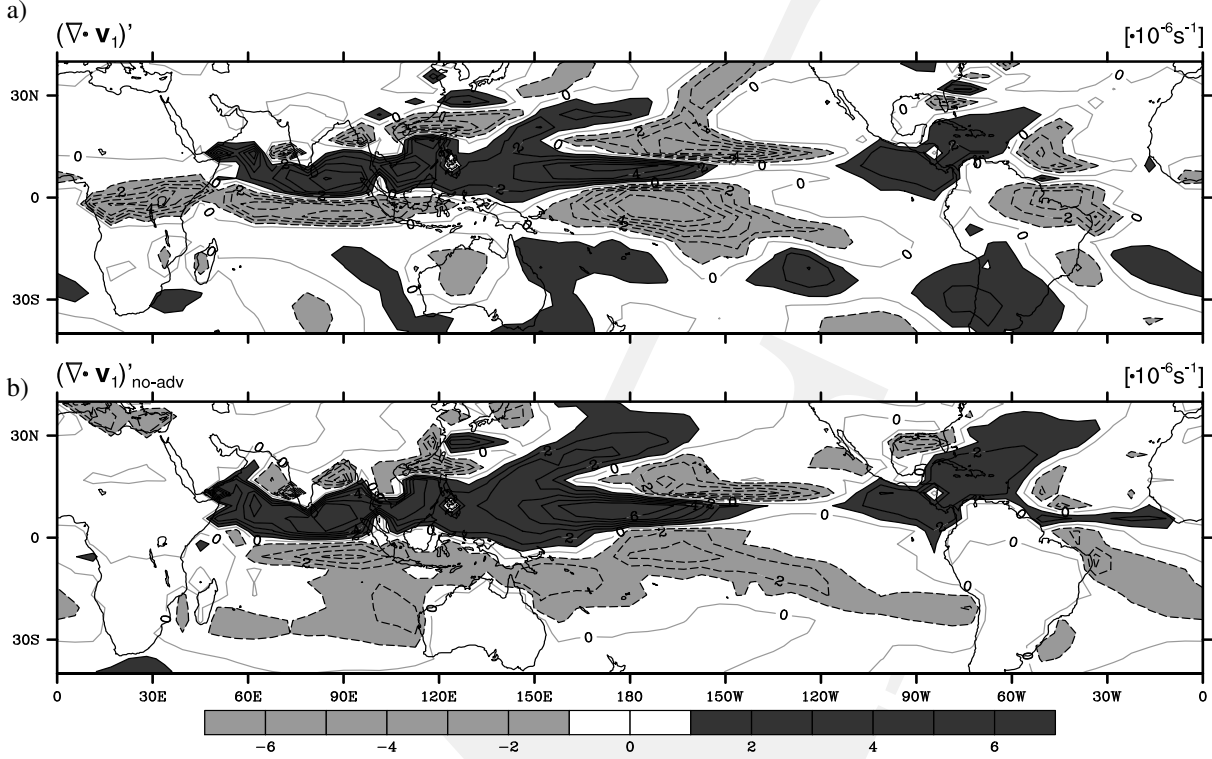


FIGURE 11: Global maps of the low level convergence change $(\nabla \cdot \mathbf{v}_1)'$ between the $\tau_{sh} = 1200\text{s}$ and $\tau_{sh} = 200000\text{s}$ run, both model and that "predicted" by (26).

has to do in order to overcome the vertical dry static energy gradients, taking into account partial cancellation by heating associated with moisture convergence. Units here follow Neelin and Su (2005). The right hand side of (23) is the net flux of energy into the column F'_{net} , where F'_{rad} is the net radiative flux (both longwave and shortwave), and E and H are the surface latent and sensible heat fluxes respectively. Equation (23) is a useful tool to express the impacts of any process affecting the column-average thermodynamics on the large scale circulation.

Figure 9 shows the individual terms in (23) at two different locations, one in the tropics and one in the subtropics. In the core of the convection zone there are two dominating terms,

$$(M\nabla \cdot \mathbf{v}_1)' \approx F'_{net}. \quad (24)$$

while in the subtropics and the margins of the convection zones $\langle D_h q \rangle'$ must be included. Expanding the perturbation terms, the change in large-scale convergence can be written

$$(\nabla \cdot \mathbf{v}_1)' = (\nabla \cdot \mathbf{v}_1)'_{no-adv} + \frac{\langle D_h q \rangle'}{M}, \quad (25)$$

$$(\nabla \cdot \mathbf{v}_1)'_{no-adv} \approx \frac{F'_{net} - M'\nabla \cdot \mathbf{v}_1^{ctl}}{M^{ctl} + M'}, \quad (26)$$

where the superscript *ctl* refers to the control run ($\tau_{sh} = 1200\text{ s}$). This equation gives the changes in large scale circulation associated with changes in surface fluxes, radiative fluxes, column-integrated moisture and moist static stability. The terms with M' were labeled by Chou and Neelin (2004) as the *M-prime mechanism*. The standard F'_{net} term is important both inside and outside the convection zones, see Fig. 9.

Figure 10 shows the change of large scale divergence in the QTCM and according to (26) in the Indian Ocean ITCZ where (26) applies well, and at a subtropical point where advection becomes important as τ_{sh} increases. Figure 11 shows maps of the divergence change $\nabla \cdot \mathbf{v}_1$ as diagnosed in the QTCM and as calculated from (26). Assumption (24) has great validity in the tropics. Figure 12 shows global maps of the terms contributing to $(\nabla \cdot \mathbf{v}_1)'$. While in the convection zones the F'_{net} term clearly dominates, the advection term can not be neglected in the subtropics (see also Fig. 9b), especially in the margins of the convection zones.

In the convection zones over the continents few increases in convergence are seen. The reason for this is that F'_{net} is small as a result of the small heat capacity of the land, yielding zero net surface flux contribution. Second, Figure 11b also shows that the continental reduc-

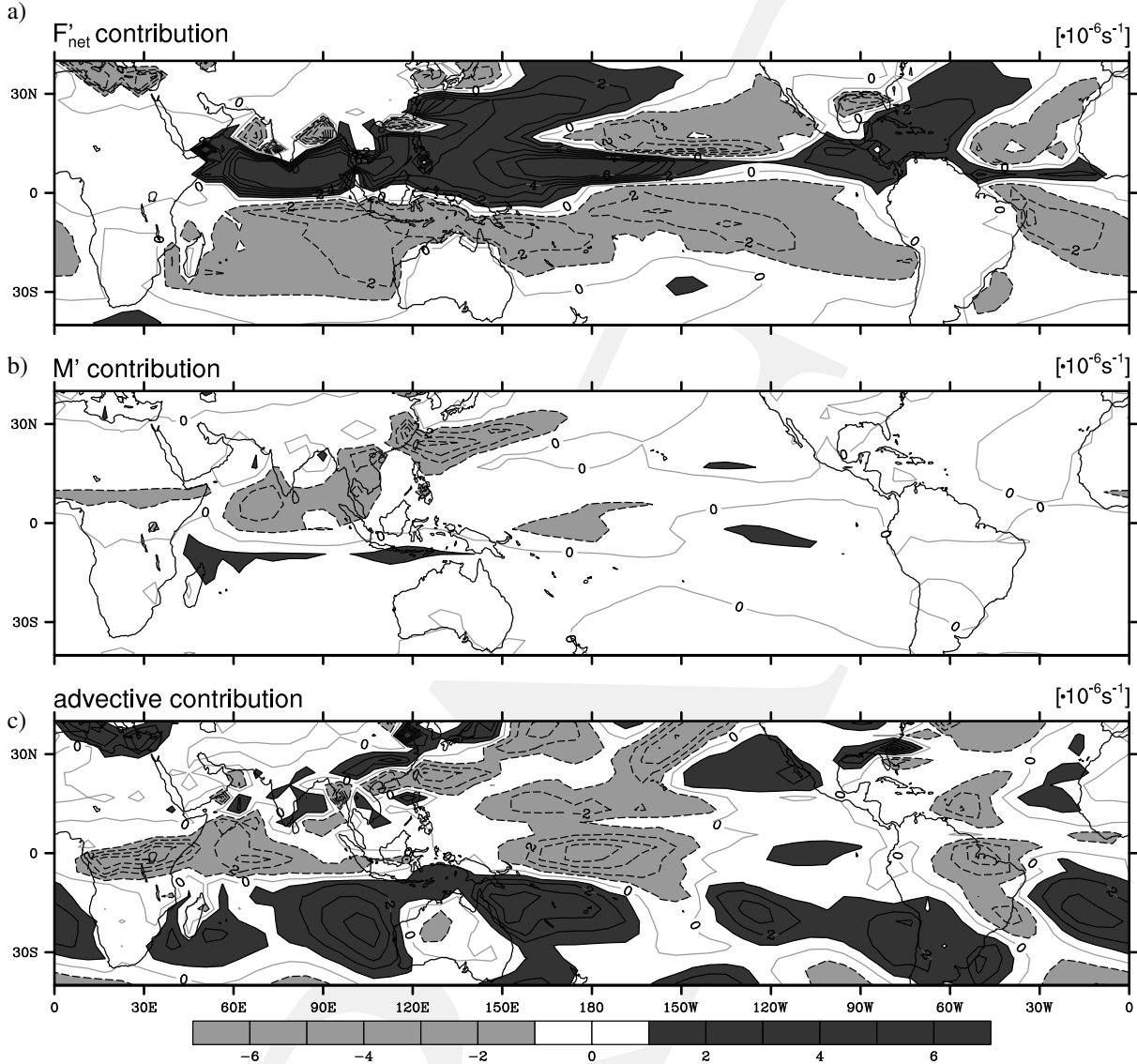


FIGURE 12: The contributions to convergence change $(\nabla \cdot \mathbf{v})'$ as plotted in Fig. 11a by a) $\frac{F'_{net}}{M^{ctl}+M'}$, b) $\frac{-M'\nabla \cdot \mathbf{v}^{ctl}}{M^{ctl}+M'}$ and c) $\frac{\langle D_h q \rangle'}{M}$. Together a) and b) make up the non-advective contribution, see (26).

tions in convergence are not well captured by (26), because the horizontal humidity advection term (Fig. 12c) causes these.

b) Net energy flux budgets

The analysis in the previous section links the changes in large scale convergence to changes in the net influx of energy into the atmospheric column. Next, a decomposition of F'_{net} is made into separate processes to determine which ones dominate. Figure 13b illustrates that in the subtropics F'_{net} is always dominated by surface evaporation. In this area shallow cumulus is the dominant type of

convection. By reducing its intensity, vertical redistribution of humidity is weakened, moistening the boundary layer, reducing the surface evaporation, and drying the lower free troposphere.

In the core of the tropical convection zones, the convection in the QTCM is always done by the deep convection scheme (see Fig. 8). As a consequence, any change in τ_{sh} does not have a local effect there, and impacts must occur through some indirect feedback mechanism. Figure 13a shows that, in contrast to the subtropics, in the convection zones two other processes are almost as important as surface evaporation in the MSE budget. These are the surface sensible heat flux H' and

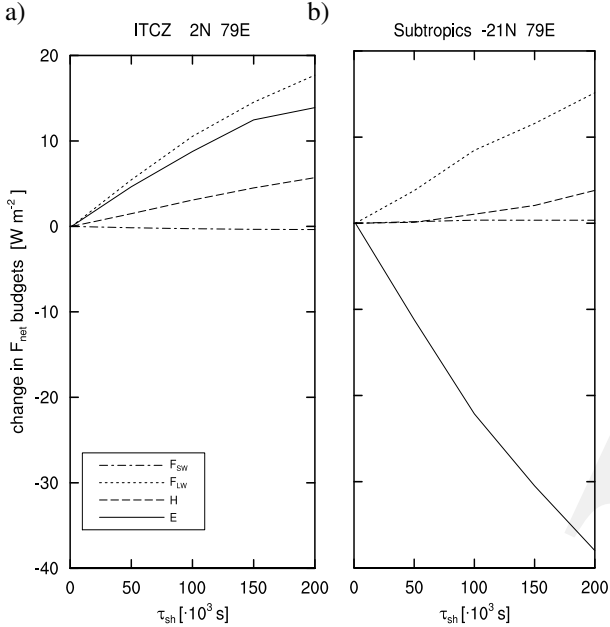


FIGURE 13: Breakdown of F'_{net} into separate processes.

the longwave radiative flux F'_{LW} . These terms suggest that a temperature change plays a role here, which is confirmed by Fig. 14. The drop in tropically averaged temperature in the latitude band between 35S and 35N is about 1 – 2 K. The similar sign and magnitude of these two terms in the subtropics reflects that this cooling is not confined to the ITCZ but manifests itself throughout a large area via equatorial wave dynamics, as expected (Neelin and Held 1987; Sobel and Bretheron 2000).

c) Convective heating

There are two ways to see the balances that lead to the temperature drop. One is that, averaged over the tropics, the transport terms in the MSE budget (23) tend to become small, so the reduction in evaporation seen in Fig. 3b must be balanced by a reduction in longwave radiation loss to the column (see Fig. 13), necessitating a temperature reduction. Alternately, we can consider the temperature equation, including the convective heating term Q_c ,

$$[\langle \partial_t T \rangle'] + [\langle \mathcal{D}_T T \rangle'] + [(M_s \nabla \cdot \mathbf{v}_1)'] = [\langle Q_c \rangle' + H' + F'_{LW} + F'_{SW}]. \quad (27)$$

Here the brackets $[\]$ denote the area-average over the latitude band between 35S and 35N. The reason for this area-averaging here is that the temperature change acts throughout the whole tropics, and therefore also the longwave radiation and surface heat flux feedbacks: a closed energy budget requires an average over the whole

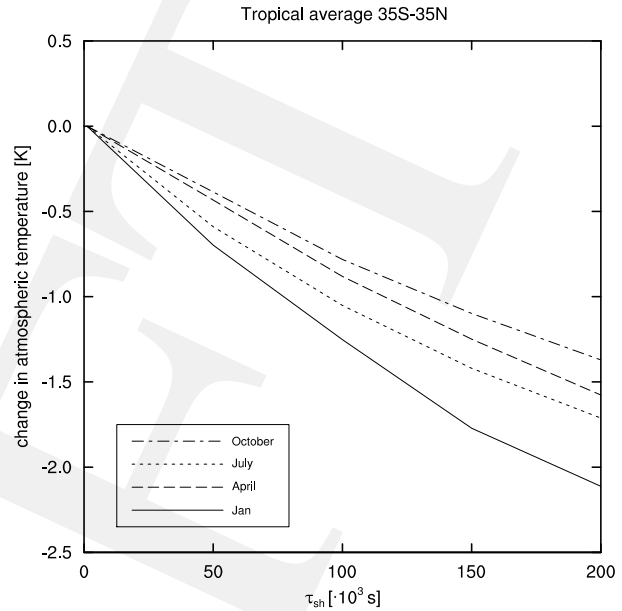


FIGURE 14: The change of the tropically averaged temperature during the sensitivity test.

area which is affected. The precipitation rate is represented in this equation by the vertically integrated convective heating tendency $\langle Q_c \rangle$.

Figure 15a shows that the change in convective heating, corresponding to a reduction in tropically averaged precipitation, is balanced largely by a reduction in long wave cooling, plus a smaller increase in the surface sensible heat flux. Figure 15b shows a further breakup of the change of the net longwave flux into contributions by temperature, moisture, surface temperature and cloud fraction (Neelin and Zeng 2000; Su et al. 2003). The main contributors are the lower tropical temperature, as well as a subtropical net moisture greenhouse effect due to the free tropospheric humidity drop.

d) Response of the large scale dynamics

At this point some conclusions can be drawn regarding the feedback mechanism that is at work. If subtropical shallow cumulus convection is reduced, the tropically averaged precipitation decreases through tropospheric advection of drier air into the ITCZ area. The associated reduction in convective heating triggers a temperature drop of about 1 – 2K throughout a large area of the tropics. In turn, this causes compensating changes in LW radiation.

Finally we return to the combined effect of all these on the overall tropical energy budget, considering the MSE budget equation (23) averaged over 35S to 35N. Figure 15c shows that decreased evaporation is indeed largely

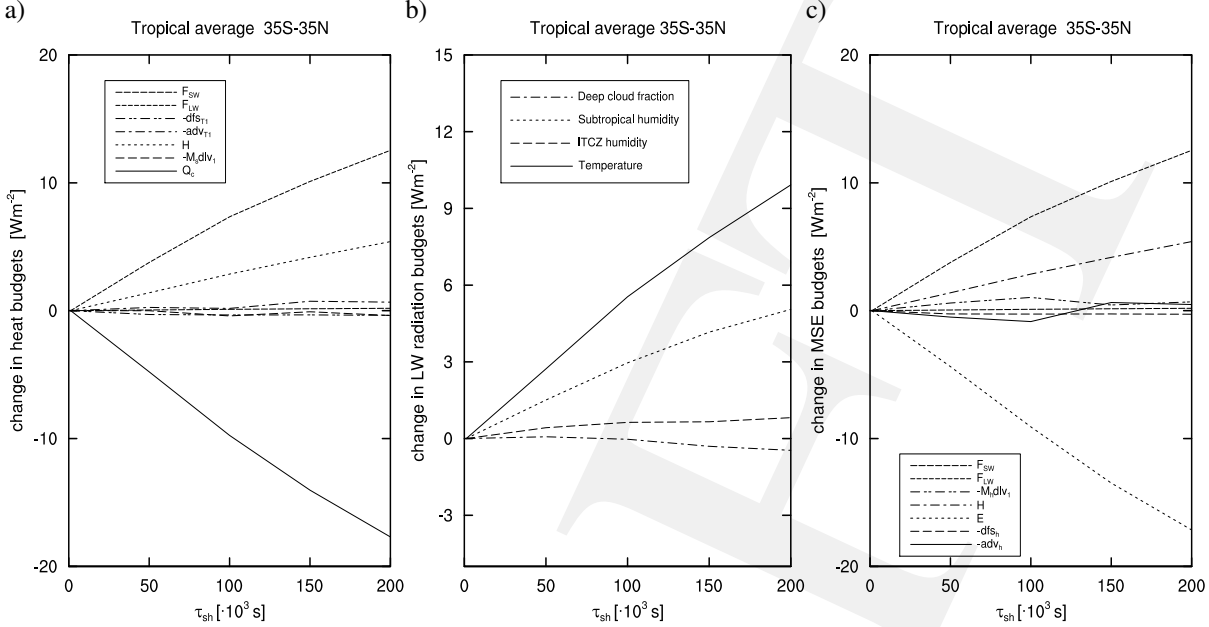


FIGURE 15: Changes in the tropically averaged (35S-35N) budgets of a) heat, b) the longwave radiative flux, and c) MSE. Changes as a function of τ_{sh} are relative to the $\tau_{sh} = 1200$ s control run. The acronyms are explained in the text. The humidity contribution to the LW radiation budget in b) is broken down into two terms representing the areas separated by the precipitation isoline of 200Wm^{-2} . These can be thought of as the convection zone and the subtropics.

balanced by the reduction in longwave cooling plus a small increase in the surface sensible heat flux. Comparing the value of the change in evaporation to the change in convective heating as plotted in Fig. 15a, we see that the tropical average precipitation change is balanced by the evaporation change.

These changes in the net energy budget of the atmosphere represent an important shift in the climatological balance between physical processes. The main loss of energy input is caused by the reduced surface evaporation, dominated by the subtropics and directly caused by the weaker shallow convection. Eventually, through many processes, this gets compensated by an enhanced input of energy through the LW radiative budget. On the way, the thermodynamic state of the tropical climate has changed significantly, with temperature changes of $1 - 2$ K and water vapour path changes of up to 10 mm.

At this point we can finally explain the changes in the large scale circulation shown earlier. To this purpose we go back to the perturbation equations (25)-(26). The temperature drop throughout the whole tropics triggers a compensating positive F'_{LW} and H' everywhere. In the core of the convection zones this causes a positive F'_{net} (Fig. 12a and Fig. 13a). As the column water vapour path has not changed that much in these areas, M is rather constant. The horizontal moisture advection can be neglected in the central parts of the convection zone. Through (26) this results in a stronger low-level

convergence, accompanied by heavier precipitation and an associated surface evaporation increase.

In the subtropics and the edges of the ITCZ, things are different. There F'_{net} is negative, as it is dominated by the evaporation decrease due to the more humid boundary layer as a result of the reduced shallow convective mixing (Fig. 13b). The associated strong decrease in subtropical water vapor path causes the M' term in (26) to be no longer negligible compared to F'_{net} (Fig. 12b). Furthermore, strong moisture gradients cause substantial drying by advection in the margins of the convection zones (Fig. 12c). Through (25) this results in less strong low-level convergence at the edges, accompanied by a lower precipitation rate.

Summarizing this analysis, the whole chain of feedbacks couples the intensity of shallow convection in the subtropics to the width and intensity of the ITCZ. The results show that this impact can be significant, with precipitation rate changes of up to 4 mm/day. The key element in this chain of feedbacks is the sensitivity of deep convection to free tropospheric humidity. Thus the Cu-q throttle launches the entire chain.

e) Oceanic mixed layer case

In the model experiments discussed so far the SST was prescribed. In reality, the oceanic mixed layer temperature is affected by the atmosphere through the net energy

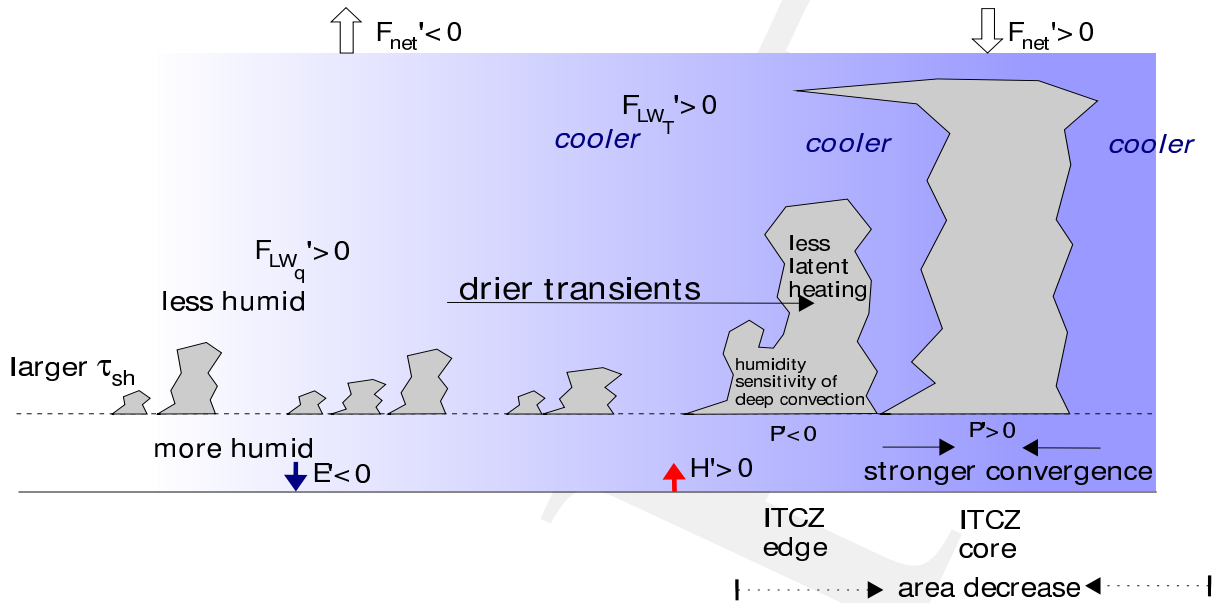


FIGURE 16: Schematic summary of the interaction mechanisms between subtropical shallow cumulus and ITCZ deep convection, the Cu-q throttle. Except for the dry transients vector, the arrows represent changes related to a larger shallow adjustment timescale τ_{sh} (weaker shallow cumulus). The background shading represents the magnitude of the temperature change.

flux at the ocean surface. The SST adjusts in such a way that the net heat flux is reduced except in regions where seasonal heat storage in the ocean is large. Examples are the areas which are only covered by an ITCZ during parts of the year, associated with its meridional seasonal migration.

In order to evaluate the impacts of an interactive SST, the same series of runs is performed but now including an interactive oceanic mixed layer of 50 m depth, as described by Su et al. (2001). The so-called Q-flux, representing the divergence of ocean heat transport, is obtained from a reference run using the method of Hansen et al. (1988). This particular Q-flux climatology is assumed to be independent of τ_{sh} , and is thus applied in all the runs.

The results (not shown) indicate that the feedback mechanism presented in the previous sections significantly affects the oceanic mixed layer temperature. For increasing τ_{sh} , the SST warms by about 2K in the subtropics, as a result of the reduced surface evaporation that dominates the surface net heat flux in those areas. Concerning the feedback mechanism discussed earlier, in the equinox seasons (MAM and SON) the strengthening of the ITCZ with reduced shallow cumulus somewhat weakens. Due to the adjustment of SST, the response in the surface heat flux and longwave radiation budget are smaller compared to the fixed SST runs. However, in the solstice seasons (JJA and DJF), in those areas which have large seasonal heat storage the SST does not adjust

fast enough to counteract the atmospheric temperature change, and the ITCZ strengthening is comparable to the fixed SST runs.

8. Discussion and conclusions

In this study a simple framework for shallow cumulus convection is used to explore its impact on the tropical climate system. The introduction of an extra degree of freedom for humidity results in two new types of convection in the QTCM: in addition to deep convection, shallow cumulus and weakly precipitating cumulus congestus occur, both of which moisten the lower troposphere. Despite the simple formulation of the convection scheme, considerable sensitivity to free tropospheric moisture is introduced, as found in cloud resolving models (Derbyshire et al. 2004). The model thus captures enough of the convective physics to assess first-order impacts on climate that could a priori be associated with the shallow cumulus humidity throttle mechanism. The decoupling of boundary layer and tropospheric humidity also increases horizontal humidity transients in the QTCM. In general, the 2BF QTCM framework can be used to study many boundary layer feedbacks on climate, for example impacts of stratocumulus clouds.

The moist static energy (MSE) framework again proves useful for studying climate feedback mechanisms. In this case, the changes in the net energy budget result directly or indirectly from changes in the intensity

of subtropical shallow convection. Shifts occur in MSE transport terms, radiative and evaporative fluxes as the large scale circulation adjusts to a new equilibrium in response to changes in shallow convection.

Figure 16 schematically summarizes these processes. Because an important step is the control over the supply of moisture to the convergence zones, we term this the shallow cumulus humidity throttle mechanism. Starting with the intensity of shallow convection in the subtropics, it ends with the width and strength of the oceanic ITCZs. When subtropical shallow cumulus convection is reduced (larger τ_{sh}) the subcloud PBL remains more humid, while the free troposphere gets significantly drier. Locally, this implies less surface evaporation. In the tropically averaged MSE budget, this loss of energy input into the atmosphere has to be compensated for, in one way or another. This adjustment occurs through a remote feedback mechanism. As the less humid lower tropospheric air is advected equatorward, the precipitative convection at the edges of the oceanic ITCZs is suppressed through the sensitivity of deep convection to atmospheric humidity. This reduction in convective heating causes the temperature to decrease by a few degrees Kelvin throughout the whole tropics. The associated strong reduction in atmospheric longwave cooling and a somewhat increased surface heat flux act to enhance the net MSE forcing everywhere. While in the subtropics this compensates the initial evaporation decrease, this is not the case in the center of the convection zones. Instead, the large scale circulation adjusts by increasing the low level convergence in the ITCZs. This is accompanied by a local increase in precipitation rate.

The findings presented here provide more insight into the strong sensitivity of GCMs to shallow cumulus, as is frequently reported (e.g. Tiedtke et al. 1988; Slingo et al. 1994; Gregory 1997; Jakob and Siebesma 2003). The role of shallow convection in the climate system is twofold: i) it transfers moisture from the subcloud PBL to the lower troposphere, affecting surface evaporation, and ii) it controls the tropospheric moisture supply to the edge of the ITCZs, affecting their width and intensity. The magnitude of these impacts can not be ignored in the global budgets of energy and water. For example, the associated climatological change in tropical precipitation is on the order of several mm day^{-1} . The tropical temperature changes associated with the latent heating by precipitation are on the order of $1 - 2\text{K}$. Furthermore, the water vapour path in the subtropics is affected by as much as 10mm locally. These numbers suggest that the shallow cumulus humidity throttle needs to be accurately accounted for in GCMs. These results suggest that the representation of shallow cumulus convection has climate impacts of similar importance to the more often

studied impact of stratocumulus clouds on the shortwave radiation budget,

A logical next question is what these results imply for GCMs in which parts of this feedback mechanism are not represented well. For example, Derbyshire et al. (2004) showed that many present-day GCM convection schemes still do not fully capture the sensitivity of deep convection to tropospheric humidity, possibly due to deficiencies in the entrainment formulation. Underestimation of the sensitivity of deep convection to humidity not only affects local cloud properties, but results here suggest it represents also a strong bias in the net MSE forcing of the tropical climate system.

Acknowledgments This research was supported in part by National Science Foundation grants DMS-0139666 and ATM-0082529. The members of the Focused Research Group on tropical atmospheric dynamics are thanked for discussions that helped stimulate this research. We thank A. Sobel for the helpful feedback on a draft version of this paper.

APPENDIX A

Technical 2BF implementation

The introduction of a second degree of freedom for humidity in the QTCM implies an additional prognostic equation for humidity, one for the free troposphere and one for the atmospheric boundary layer ($k \in \{1, 2\}$ respectively). Following the standard notation of the QTCM formulation by NZ00 these are written as

$$\hat{b}_1(\partial_t + D_{q1})q_1 - M_{1q1}\nabla \cdot \mathbf{v}_1 = \langle Q_q \rangle_1 \quad (\text{A1})$$

$$\hat{b}_2(\partial_t + D_{q2})q_2 - M_{1q2}\nabla \cdot \mathbf{v}_1 = \langle Q_q \rangle_2 + \frac{g}{P_2}E_s \quad (\text{A2})$$

The terms M_{1qk} represent the gross moisture stratification for vertical motions induced by large-scale convergence of the baroclinic wind \mathbf{v}_1 in layer k (note that the subscript 1 in M_{1qk} and v_1 refers to the basis functions for wind, which differ from those for humidity). The two prognostic humidity equations are coupled by the convective humidity tendency $\langle Q_q \rangle_k$. E_s is the surface evaporation into the relatively shallow boundary layer. Further vertical redistribution into the free troposphere depends on the convective intensity $\langle Q_q \rangle_k$, described in Section 3.

The stratification terms M_{1qk} are calculated over the depth of each layer, as a function of the internal vertical structure functions of humidity $b_k(p)$ [see (7) and

Fig.1] and of baroclinic vertical velocity $\Omega_1(p)$, defined by NZ00 as

$$\omega(p) \equiv \Omega_1(p) \nabla \cdot \mathbf{v}_1. \quad (\text{A3})$$

This gives

$$M_{1qk} = \langle \Omega_1 \partial_p q_r \rangle_k + \sum_{j=1}^2 \langle \Omega_1 \partial_p b_j \rangle_k q_j, \quad (\text{A4})$$

$$\equiv M_{1q_r k} + M_{1q_p k} \quad (\text{A5})$$

where q_r is the reference humidity profile, a function only of pressure. In each layer both BFs contribute to the last term on the right hand side, due to their small overlap at p_m . This overlap can be used for the formulation of either centered or upwind schemes for vertical advection. Suppose the overlap layer spans the pressure depth $\langle p_m - \epsilon_1, p_m + \epsilon_2 \rangle$ where $\epsilon_1 + \epsilon_2 = \epsilon$. The last term of (A5) then consists of a bulk integral and an integral over a part of the overlap layer,

$$M_{1q_p k} \equiv M_{1q_p k}^{bulk} + M_{1q_p k}^{int}. \quad (\text{A6})$$

Working out the interface term, using linear gradients of the structure functions $b_k(p)$ in the overlap layer, gives

$$M_{1q_p k}^{int} = \frac{\Omega_1(p_m)}{P_k} (b_2^- q_2 - b_1^+ q_1) \frac{\epsilon_k}{\epsilon}, \quad (\text{A7})$$

where the superscripts $+$ and $-$ refer to the values of the structure function immediately above and below the overlap layer. Furthermore, ϵ is assumed to be sufficiently small so that $\Omega_1(p)$ can be assumed constant in the overlap layer. For a centered advection scheme, set $\epsilon_1 = \epsilon_2 = \frac{1}{2}\epsilon$. For an upwind scheme, the last step is to make p_m dependent on model state. In subsidence conditions, p_m is chosen such that $\epsilon_2 = \epsilon$, $\epsilon_1 = 0$, in effect including the overlap layer in layer 2. In convergence conditions, $\epsilon_1 = \epsilon$, $\epsilon_2 = 0$. As a result, downward advection by large scale subsidence dries the boundary layer when a humidity jump exists at the mixed layer top. This corresponds to top entrainment of air into the convective boundary layer.

REFERENCES

- Betts, A. K., 1975: Parametric interpretation of Trade-wind cumulus budget studies. *J. Atmos. Sci.*, **32**, 1934-1945.
- , 1986: A new convective adjustment scheme. Part I: Observational and theoretical basis. *Quart. J. Roy. Met. Soc.*, **112**, 677-691.
- , and M. J. Miller, 1986: A new convective adjustment scheme. Part II: Single column tests using GATE wave, BOMEX, ATEX and arctic air-mass data sets. *Quart. J. Roy. Met. Soc.*, **112**, 693-709.
- Chou, C. and J. D. Neelin, 2004: Mechanisms of global warming impacts on regional tropical precipitation. *J. Clim.*, **17**, 2688-2701.
- Derbyshire, S. H., I. Beau, P. Bechtold, J.-Y. Grandpeix, J.-M. Piriou, J.-L. Redelsperger and P. M. M. Soares: Sensitivity of moist convection to environmental humidity. *Q. J. Roy. Met. Soc.*, **130**, 3055-3079.
- Gregory, D., 1997: Sensitivity of general circulation model performance to convective parameterization. *The Physics and Parameterization of Moist Atmospheric Convection*, edited by R. K. Smith. NATO ASI Series C, **505**, Kluwer Academic Publishers.
- Hansen, J., I. Fung, A. Lacis, D. Rind, S. Lenedeff, et al., 1988: Global climate changes as forecast by Goddard Institute for Space Studies three-dimensional model. *J. Geophys. Res.* **93D**, 9341-9364.
- Jakob, C., and A. P. Siebesma, 2003: A new subcloud model for mass-flux convection schemes; Influence on triggering, updraft properties and model climate. *Mon. Wea. Rev.*, **131**, 2765-2778.
- Johnson, R. H., T. M. Rickenbach, S. A. Rutledge, P. E. Ciesielske and W. H. Schubert, 1999: Trimodal characteristics of tropical convection. *J. Climate*, **12**, 2397-2418.
- Lin, J. W.-B., J. D. Neelin and N. Zeng, 2000: Maintenance of tropical intraseasonal variability: impact of evaporation-wind feedback and midlatitude storms. *J. Atm. Sci.*, **57**, 2793-2823.
- Liu, W. T., W. Tang and P. P. Niiler, 1991: Humidity profiles over the ocean. *J. Clim.*, **4**, 1023-1034.
- Neelin, J. D., and I. M. Held, 1987: Modeling tropical convergence based on the moist static energy budget. *Mon. Wea. Rev.*, **115**, 3-12.
- , and N. Zeng, 2000: A quasi-equilibrium tropical circulation model - formulation. *J. Atmos. Sci.*, **57**, 1741-1766.
- , C. Chou, and H. Su, 2003: Tropical draught regions in global warming and El Nino teleconnections. *Geophys. Res. Lett.*, **30**, 2275, doi:10.1029/2003GL018625.
- , and H. Su, 2005: Moist teleconnection mechanisms for the tropical south american and atlantic sector. *J. Clim.*, **18**, 3928-3950.
- Neggers, R. A. J., B. Stevens, and J. D. Neelin: A simple equilibrium model for shallow cumulus topped mixed layers. *Submitted to Theor. and Comp. Fluid Dyn.*, August 2005.
- Newell, R. E., N. E. Newell, and C. Scott, 1992: Tropospheric rivers?—A pilot study. *Geophys. Res. Lett.*, **19**, 2401-2404.
- , and Zhu, Y. 1994: Tropospheric rivers: A one-year record and a possible application to ice core data. *Geophys. Res. Lett.*, **21**, 113-116.
- Ooyama, K., 1971: A theory on parameterization of cumulus convection. *J. Meteor. Soc. Japan*, **49**, 744-756.
- Parsons, D. B., K. Yoneyama and J.-L. Redelsperger, 2000: The evolution of the tropical western Pacific ocean-atmosphere system following the arrival of a dry intrusion. *Q. J. Roy. Met. Soc.*, **126**, 517-548.
- Pierrehumbert, R. T. and H. Yang, 1993: Global chaotic mixing on isentropic surfaces. *J. Atmos. Sci.*, **50**, 2462-2480.
- Riehl, H., C. Yeh, J. S. Malkus, and N. E. LaSeur, 1951: The northeast trade of the Pacific Ocean. *Quart. J. Roy. Meteor. Soc.*, **77**, 598-626.
- Siebesma, A. P., and Cuijpers, 1995: Evaluation of parametric assumptions for shallow cumulus convection. *J. Atmos. Sci.*, **52**, 650-666.
- Slingo, J. M., M. Blackburn, A. Betts, R. Brugge, B. J. Hoskins, M. J. Miller, L. Steenman-Clark and J. Thurburn, 1994: Mean climate and transience in the tropics of the UGAMP GCM: Sensitivity to convective parameterization. *Quart. J. Roy. Met. Soc.*, **120**, 881-922.
- Sobel, A. H., and C. S. Bretherton, 2000: Modeling tropical precipitation in a single column. *J. Climate*, **13**, 4378-4392.
- Su, H., J. D. Neelin, and C. Chou, 2001: Tropical teleconnection and local response to SST anomalies during the 1997-1998 El Niño. *J. Geophys. Res.*, **106**, 20025-20043.
- , and ———, 2002: Teleconnection mechanisms for tropical Pacific descent anomalies during El Niño. *J. Atmos. Sci.*, **59**, 2682-2700.
- , ———, and J. E. Meyerson, 2003: Sensitivity of tropical tropospheric temperature to sea surface temperature forcing. *J. Clim.*, **16**, 1283-1301.
- , and ———, 2003: The scatter in tropical average precipitation anomalies. *J. Clim.*, **16**, 3966-3977.
- Tiedtke, M., W. A. Heckley and J. Slingo, 1988: Tropical forecasting at ECMWF: The influence of physical parameterizations on the mean structure of forecasts and analyses. *Quart. J. Roy. Met. Soc.*, **114**, 639-665.

- Yanai, M., S. Esbensen and J.-H. Chu, 1973: Determination of bulk properties of tropical cloud clusters from large-scale heat and moisture budgets. *J. Atmos. Sci.*, **30**, 611-627.
- Zeng, N., J. D. Neelin and C. Chou, 2000: A quasi-equilibrium tropical circulation model - Implementation and simulation. *J. Atmos. Sci.*, **57**, 1767-1796.

DRAFT